agriculture

MDPI

Article

Research on the Three-Level Integrated Environmental Evaluation Model for Multi-Greenhouse Potatoes

Shize Liu [1], Tao Zhong [2], Huan Zhang [1], Jian Zhang [2], Zhiguo Pan [1] and Ranbing Yang [2,*]

[1] College of Mechanical and Electrical Engineering, Qingdao Agricultural University, Qingdao 266109, China; 20212204007@stu.qau.edu.cn (S.L.); 200501102@qau.edu.cn (H.Z.); 200701031@qau.edu.cn (Z.P.)
[2] College of Mechanical and Electrical Engineering, Hainan University, Haikou 570228, China; 21220951360017@hainanu.edu.cn (T.Z.); 200601168@qau.edu.cn (J.Z.)
* Correspondence: yangranbing@163.com

Abstract: Aiming at the problems of large error and redundancy in the multi-node data acquisition of multi-greenhouse photo growth environmental information, a three-level fusion algorithm based on adaptive weighting, an LMBP network, and an improved D-S theory is proposed. The box-and-line graph method recognizes the original data and then replaces it based on the mean value method; the air temperature, humidity, and light intensity measurements are unbiased estimations of the true value to be estimated, so the first level of fusion chooses the adaptive weighted average algorithm to find the optimal weights of each sensor under the condition of minimizing the total mean-square error and obtains the optimal estimation of the weights of the homogeneous sensors of a greenhouse. The Levenberg–Marquardt algorithm was chosen for the second level of fusion to optimize the weight modification of the BP neural network, i.e., the LMBP network, and the three environmental factors corresponding to "suitable", "uncertain" and "unsuitable" potato growth environments were trained for the three environmental factors in the reproductive periods. The output of the hidden layer was converted into probability by the Softmax function. The third level is based on the global fusion of evidence theory (also known as D-S theory), and the network output is used as evidence to obtain a consistent description of the multi-greenhouse potato cultivation environment and the overall scheduling of farming activities, which better solves the problem of the difficulty in obtaining basic probability assignments in the evidence theory; in the case of a conflict between the evidence, the BPA of the conflicting evidence is reallocated, i.e., the D-S theory is improved. Example validation shows that the total mean square error of the adaptive weighted fusion value is smaller than the variance of each sensor estimation, and sensors with lower variance are assigned lower weights, which makes the fusion result not have a large deviation due to the failure of individual sensors; when the fusion result of a greenhouse feature level is "unsuitable", the fusion result of each data level is considered comprehensively, and the remote control agency makes a decision, which makes full use of the complementary nature of multi-sensor information resources and solves the problem of fusion of multi-source environmental information and the problem of combining conflicting environmental evaluation factors. Compared with the traditional D-S theory, the improved D-S theory reduces the probability of the "uncertainty" index in the fusion result again. The three-level fusion algorithm in this paper does not sacrifice data accuracy and greatly reduces the noise and redundancy of the original data, laying a foundation for big data analysis.

Keywords: greenhouse; potato; environmental evaluation; adaptive weighting; BP neural network; D-S theory

Citation: Liu, S.; Zhong, T.; Zhang, H.; Zhang, J.; Pan, Z.; Yang, R. Research on the Three-Level Integrated Environmental Evaluation Model for Multi-Greenhouse Potatoes. *Agriculture* **2024**, *14*, 1043. https://doi.org/10.3390/agriculture14071043

Academic Editors: Miltiadis Iatrou, Christos Karydas and Panagiotis Tziachris

Received: 3 May 2024
Revised: 24 June 2024
Accepted: 25 June 2024
Published: 29 June 2024

1. Introduction

In 2015, China launched a strategy to make potato a staple food, ranking it alongside rice, wheat and maize as one of the four major staples. A well-managed potato crop yields up to 60,000 kg per ha, while a poorly managed one yields less than 15,000 kg,

and unsuitable conditions at any given time can result in yield reductions [1]. In order to improve the yield and quality of potatoes, greenhouse cultivation is commonly used today. The environment inside the greenhouse is related to the absorption of organic matter and energy conversion, and the use of supporting facilities to regulate the greenhouse environment so that it always meets the needs of potato growth can achieve very high economic benefits in large-scale continuous greenhouses [2].

Traditional greenhouse control systems use a single-threshold method. If the temperature exceeds a limit, the system cools based on sensor data [3–5]. However, changing one environmental factor often affects others, making it hard to control the greenhouse accurately. Also, a single sensor's information does not account for variations in the greenhouse, and sensor accuracy decreases over time [6]. In summary, the environmental information of a point in the greenhouse cannot be used as the basis for decision-making. Potato growth is cross-influenced by many factors. To accurately control the environmental information from multiple greenhouses with the help of a large number of sensors, the type and number of sensors need to be increased, but with the increase in the number of sensors, the data from the same greenhouse is captured by multiple sensors, resulting in data redundancy [7]. How to effectively monitor the greenhouse environment in real time is always a problem; multi-sensor information fusion can analyze and synthesize data from multiple monitoring sensors [8–10]. It is necessary to introduce this technology into the greenhouse potato growth environment assessment.

The fusion of multi-source environmental information is developing rapidly, and there is a wealth of algorithms for users to choose from [11]. After evaluating the performance of PM2.5 prediction with AOD data, Mirzaei Ali et al. [12] chose the XGBoost algorithm as the base model for multilevel fusion, which improved the accuracy of PM2.5 prediction.

Adaptive weighted average algorithm is the classic algorithm for fusing homogeneous sensors in a region, but it is easy to appear the case that the fusion value of successive times is close to the mean value. At this time, the advantages of adaptive weighting algorithm cannot be reflected, and it needs to be preprocessed by algorithms such as Dixon criterion and wavelet noise reduction to improve the fusion accuracy of adaptive weighting algorithm [13].

Multi-point sensors are installed in the greenhouse to avoid the problem of inaccurate measurement of single sensors, and the adaptive weighting algorithm fusion is combined with a back propagation (BP) network to judge the trends in the parameters to make decisions on the control scheme. The second-level fusion, consisting of adaptive weighting and a BP network, provides for a good greenhouse growing environment, but the second-level fusion results of different greenhouses have large differences, which is not conducive to the overall scheduling of potato farming activities in continuous greenhouses. The evidence theory (also known as the D-S theory) is chosen as the third level of fusion to obtain a consistent description of the results of the environmental evaluation of multiple greenhouses in the same time period, which helps to arrive at the optimal environmental control program.

In order to address the problems of multiple greenhouses relying on single-factor ring control and redundant environmental data, in this paper, we first preprocessed the raw data based on the box-and-line diagram method, adaptively weighted the fusion of similar sensor data with a constant estimation value, and trained the BP network in the reproductive period, thus improving the D-S theory to reduce the uncertainty of the results. After completing the three-level fusion, the third-level fusion results represent a consistent description of the potato planting situation at the base; based on the results of the first two levels of fusion, the actuator devices are controlled to simulate the appropriate growing environment in each greenhouse, which is more reliable than a single sensor.

2. Materials and Methods

2.1. Potato Growth in Relation to Environmental Factors

Potatoes have unique requirements for environmental conditions at all stages of fertility [14], and these conditions determine whether high yields can be achieved. Some of the environmental factors that have a greater impact on growth are listed below.

1. Air temperature. Potatoes like cold, though it is important to avoid frost, and high temperatures should be avoided. Temperature is the main limiting factor of their growth. Potato stem and leaf growth and expansion of its tubers have different air temperature requirements. When the indoor air temperature is higher than 5 °C and the ground (10 cm) temperature is consistently higher than 0 °C, they can be sown. The stem and leaf grow best at 17–21 °C [15].
2. Air humidity. Relative humidity is commonly used to express the amount of humidity in the air. The annual average relative humidity in Qingdao is about 73%, which is relatively high, with an average of about 70% RH from April to June and an average of about 66% RH from December to February. Compared with the field, the airflow inside the greenhouse is relatively stable, the potato metabolism is fast—releasing a large amount of water vapor—and the air humidity is higher; too little air humidity will affect the water balance in the plant and weaken photosynthesis.
   Potato water demand and evapotranspiration are closely related. They should be based on potato production needs; good water control is needed to provide suitable environmental conditions for potato growth. For example, drip irrigation can reduce the air temperature and raise air humidity. Affected by irrigation and the temperature difference between day and night, the shed is prone to excessive humidity; therefore, pay attention to air release at noon during the day to reduce humidity.
3. CO_2 concentration. CO_2 is the raw material for photosynthesis, and CO_2 content induces potato photosynthesis to manufacture nutrients, which can increase the photosynthesis light saturation point and is conducive to the accumulation of potato nutrients. The CO_2 content of the air in the shed reaches 0.1%, which is very favorable for potato growth [16].
4. Light intensity. Potato is a light-loving crop; it is sensitive to light, with more than 90% of the dry matter in the body being the product of photosynthesis. The light saturation point of potatoes is 30,000–40,000 lx, and the intensity of photosynthesis is the highest in this range. Only by meeting the demand for light during potato development will the crop be of good quality and high yield. The energy required for potato growth comes mainly from sunlight, followed by various artificial light sources. Japan's Nakashigu Gongnan at Hokkaido University reduced light intensity to 75%, 53%, and 30% of natural light, then measured the total dry matter weight with the reduction of light intensity; when light intensity was reduced to 30% of natural light, the dry weight of the yield was reduced by 60% to 67% [17,18].

Day length, light intensity, and temperature have mutual effects on the potato fertility period. To increase production, the most suitable conditions for the seedling period are short light, strong light, and appropriate high temperature; for the tuber formation period, long light, strong light, and appropriate high temperature; for the tuber expansion period and starch accumulation period, short light, strong light, and appropriate low temperature. Greenhouse potato growth and development in short light and strong light conditions can extend the effective growth period of potatoes, conducive to the formation and expansion of tubers.

2.2. Basic Information Regarding the Base

Jiaolai Town, Jiaozhou City, Qingdao, Shandong Province, has a warm temperate monsoon continental climate with four distinct seasons and little rain in spring and fall. Dazhaojia Village has a "national key project demonstration base for potato intelligent production equipment", where potatoes are mostly grown in greenhouses with drip irrigation

in order to improve yield and quality. Compared with field potatoes, which are susceptible to frost, the intelligent greenhouse creates a relatively stable ecological environment. Sensors monitor indoor environmental information in real time with a sampling frequency of 1 min and send it to the IoT cloud platform.

The greenhouse control cabinet monitors water and fertilizer information and environmental information. It integrates, analyzes, processes, and stores the environmental digital information collected by the water–fertilizer integration control terminal and remotely controls the actuators to complete the optimization of environmental parameters. The actuators are as follows:

1. Humidification equipment. High-pressure atomization equipment spraying ultra-micro-fog particles. The heat absorption and cooling effect is obvious and can effectively supplement the potato due to transpiration caused by the lack of moisture.
2. Shading equipment. In the shed, the roller shutter insulation material reduces heat loss in the greenhouse when the outdoor temperature is low and helps to maintain the indoor temperature in the appropriate range. The rolling curtain machine is mainly composed of an electric motor, a reducer, and a rolling curtain shaft. By adjusting the opening degree of the roller shutter, the outdoor temperature is used to make the potato accept more light, realize daytime light transmission, and provide night insulation.
3. Ventilation equipment. Restricted by the interior space of the greenhouse, the airflow is more stable. If the ventilation is not timely, the indoor air is easily saturated with water vapor. Especially at night, if the outdoor temperature is low and the indoor humidity is high, the resulting mist makes the leaves dewy, and it is easy to cause late blight and other diseases. The electric film winder quickly rolls and releases the shed film, freely adjusts the area of the vents, and realizes the release of wind and dehumidification.

The rolling range of the rolling curtain is the whole surface of the shed, and the rolling range of the rolling film is from the top of the shed and the bottom of the shed along the surface of the extension of a distance. The remaining range of the rolling thermal insulation quilt, the thermal insulation quilt, and the rolling range of the rolling film complement each other. When the rolling curtain is closed, the rolling film is always closed; according to the environmental conditions, the opening degree of the rolling curtain and the rolling film is controlled.

2.3. Integration Programming

The greenhouse potato growth environment is affected by many factors, such as the flowering period, which requires an average daily temperature of 18–20 °C, air humidity of 80% to 90%, and at least 12 h of long sunshine per day [19]. In order to simplify the calculation, the air temperature, humidity, and light intensity, which have a greater impact, were selected for the growth environment assessment.

Sensors collecting similar environmental factors were homogeneous sensors that were fused by adaptive weighting [20]; sensors collecting different environmental factors were heterogeneous sensors [21], which were fused by the LMBP network prediction model and improved D-S theory. Data with large differences will reduce the accuracy of the three-level fusion, which should be checked by the box-and-line plot method first, and the outliers are replaced based on the mean value method. The block diagram of the fusion structure is shown in Figure 1.

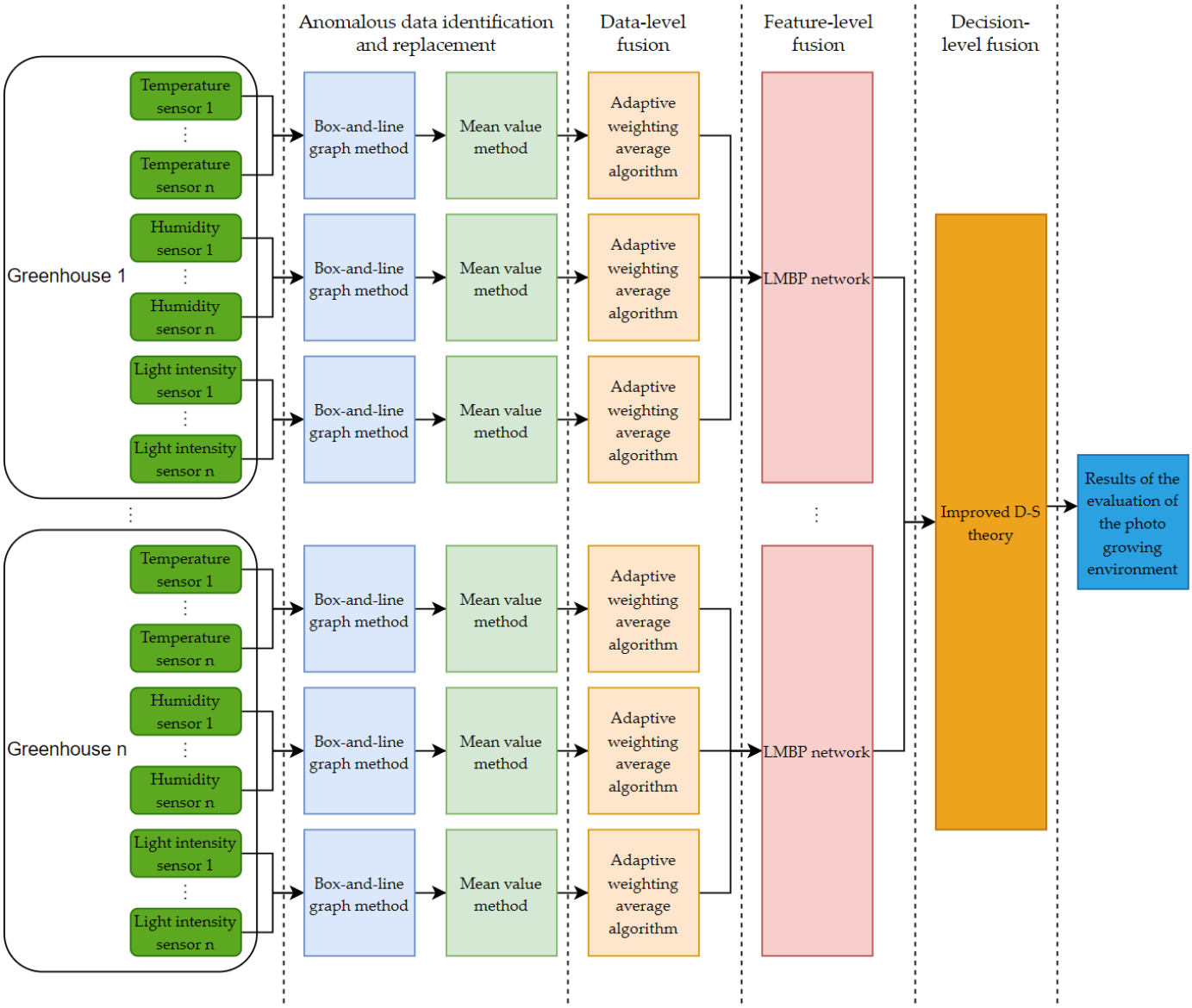

Figure 1. Modeling of multi-source data fusion for environmental monitoring of greenhouse potatoes.

Data fusion is the process of abstracting the original data [22], and the abstraction levels are, in descending order, data-level fusion, feature-level fusion, and decision-level fusion.

1. Data-level fusion. The input quantity for data-level fusion is the preprocessed data from homogeneous sensors. In the greenhouse, the sensor measurements corresponding to air temperature, humidity, and light intensity are unbiased estimates of the true value to be estimated, so an adaptive weighted average algorithm is selected in the data-level fusion process to fuse homogeneous sensor measurements in a greenhouse to reduce the uncertainty of the environment assessed by a single sensor.
2. Feature-level fusion. Feature-level fusion can use artificial intelligence, neural networks, and other theories to process data and obtain feature-level vectors of different dimensions, which can analyze the decision-making information contained in the data and prepare for decision-level fusion. The input of the LMBP network is the air temperature, humidity, and light intensity adaptive weighted fusion value of each greenhouse; the output layer selects the Softmax function, adopts the nonlinear function method, and transforms the variables of the output of the hidden layer into [0, 1] interval probability, according to the probability of high and low judgments of "suitable", "uncertain", and "unsuitable" categories. The LMBP network assigns

probabilities, taking advantage of the fast convergence of the BP algorithm. After predicting the cultivation environment of a single greenhouse with the neural network, the cause of "unsuitable" is traced back, and then the decision is made on the environmental control measures after comprehensive consideration.

3. Decision-level fusion. Decision-level fusion is the final result of the three-level fusion. Due to sensor failure and aging, system and environmental noise, and other uncertainties, a shed's feature-level fusion results cannot be used to represent the overall environmental conditions of the base. The input to decision-level fusion is the output of the feature-level fusion, i.e., the neural network outputs from multiple canopies are used as evidence for the basic probability assignments needed for D-S theory inference. If there is a conflict between the evidence, the BPA of the conflicting evidence is reassigned, i.e., the D-S theory is improved.

2.4. Anomaly Data Processing Based on Box-and-Line Diagram Method

Due to the mechanical failure and aging malfunction of the sensor itself, as well as environmental interference and other effects, it is easy to produce data with large deviations from normal values. If these data are not processed relevantly, the subsequent adaptive weighted fusion value will produce large fluctuations near these points, which will ultimately reduce the reliability of the decision-making results. In order to detect these anomalies, this paper adopts the box-and-line diagram method to preprocess the raw data [23]. The process is as follows:

Arrange the n data points obtained from the same sensor in time series from smallest to largest to get $[x_1, x_2, \ldots, x_n]$. The box-and-line plot data division is shown in Figure 2, and the data confidence interval $[\beta_p, \beta_q]$ is defined.

$$\begin{cases} \beta_p = Q_1 - 1.5IQR \\ \beta_q = Q_3 + 1.5IQR \end{cases} \tag{1}$$

where Q_1 and Q_3 are the lower and upper quartiles and IQR is the interquartile spacing:

$$IQR = Q_3 - Q_1 \tag{2}$$

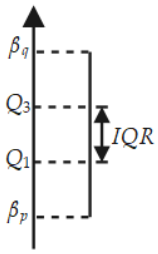

Figure 2. Boxplot data segmentation.

Values outside the interval $[\beta_p, \beta_q]$ are outliers. Upon detection of an outlier, direct deletion affects the time series continuity of the sample data, and the outlier is replaced with the mean value of the remaining data.

2.5. First-Level Fusion Based on Adaptive Weighted Average Algorithm

An adaptive weighted average algorithm is used to fuse each greenhouse with the processed homogeneous sensor data. The core idea of the algorithm is to minimize the total mean square error under the conditions of the total mean square error, according to the measurement value of each sensor, and in an adaptive way to find the optimal weighting factor corresponding to the sensor. The sensor data and the corresponding weighting factor are multiplied, and then by summing these, the fusion value can be obtained [24], as shown in Figure 3.

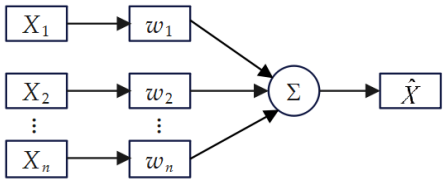

Figure 3. Adaptive weighted average algorithm model.

2.5.1. Fundamentals of the Adaptive Weighted Average Algorithm

If there are n sensors detecting a certain environmental parameter, the corresponding variances are σ_1^2, σ_2^2,. . ., σ_n^2, and the truth value to be estimated is X. The measurements of each sensor are X_1, X_2,. . ., X_n, which are independent of each other and are the unbiased estimation of X; the weighting factors of each sensor are ω_1, ω_2,. . ., ω_n, respectively, and the fused $\hat{X}$ satisfies the following relationship:

$$\begin{cases} \hat{X} = \sum_{i=1}^{n} \omega_i X_i \\ \sum_{i=1}^{n} \omega_i = 1 \end{cases} \tag{3}$$

The total mean square error σ^2 is:

$$\sigma^2 = E[(X-\hat{X})^2] = E[(\sum_{i=1}^{n}\omega_i X - \sum_{i=1}^{n}\omega_i X_i)^2] = E[(\sum_{i=1}^{n} W_i(X-X_i))^2] = E[\sum_{i=1}^{n}\omega_i\sigma^2(X-X_i)^2 + 2 \sum_{\substack{i=1, j=1 \\ i \neq j}}^{n} (X-X_i)(X-X_j)] \tag{4}$$

X_1, X_2,. . ., X_n are independent of each other and are unbiased estimates of X, then:

$$E(X-X_i)(X-X_j) = 0 \tag{5}$$

where i = 1, 2,. . ., n; j = 1, 2,. . ., n and $i \neq j$, when the total mean square error is:

$$\sigma^2 = E[\sum_{i=1}^{n}\omega_i^2(X-X_i)^2] = \sum_{i=1}^{n}\omega_i^2\sigma_i^2 \tag{6}$$

where σ_i^2 is the estimated variance of the i–th sensor. From Equation (6), σ^2 is a multivariate quadratic function with respect to the weighting factor, and σ^2 has the minimum value, which is the solution of Equation (7).

$$\begin{cases} \sigma_{\min}^2 = \min(\sum_{i=1}^{n}\omega_i^2\sigma_i^2) \\ \sum_{i=1}^{n}\omega_i = 1 \end{cases} \tag{7}$$

According to the theory of polarization of multivariate functions, the weighting factor is when the total mean square error is minimized:

$$\omega_i = 1/(\sigma_i^2\sum_{i=1}^{n}\frac{1}{\sigma_i^2}) \tag{8}$$

At this point, the total mean square error is minimized as:

$$\sigma_{\min}^2 = 1/\sum_{i=1}^{n}\frac{1}{\sigma_i^2} \tag{9}$$

When the true value of the value to be estimated is constant, it is estimated by the mean value of the historical data of each sensor [25], and the mean value of the i–th sensor measured k times is:

$$\overline{X}_i(k) = \frac{1}{k}\sum_{j=1}^{k} X_j \tag{10}$$

Estimated value:

$$\hat{\overline{X}} = \sum_{i=1}^{n} \omega_i \overline{X}_i(k) \tag{11}$$

The total mean square error is:

$$\overline{\sigma}^2 = E[\sum_{i=1}^{n} \omega_i^2 (X - \overline{X}_i(k))^2 + 2 \sum_{\substack{i=1, j=1 \\ i \neq j}}^{n} (X - \overline{X}_i(k))(X - \overline{X}_j(k))] \tag{12}$$

$X_1, X_2, \ldots, X_n$ are unbiased estimates of X. Therefore, $\overline{X}_1(k), \overline{X}_2(k), \ldots, \overline{X}_n(k)$ are also unbiased estimates of X. Equation (12) simplifies to:

$$\overline{\sigma}^2 = E[\sum_{i=1}^{n} \omega_i^2 (X - \overline{X}_i(k))^2] = \frac{1}{k}\sum_{i=1}^{n} \omega_i \sigma_i^2 \tag{13}$$

The optimal weighting factor still satisfies Equation (8) when $\overline{\sigma}^2$ is minimized, and $\overline{\sigma}^2$ is minimized as:

$$\overline{\sigma}^2_{\min} = 1/k \sum_{i=1}^{n} \frac{1}{\sigma_i^2} = \frac{\sigma^2_{\min}}{k} \tag{14}$$

Clearly, $\overline{\sigma}^2_{\min}$ is less than $\sigma^2_{\min}$, and $\overline{\sigma}^2_{\min}$ decreases with the number of measurements k.

2.5.2. Derivation of the Estimated Variance σ_i^2 for Each Sensor

From Equation (8), the estimated variance σ_i^2 of each sensor is obtained to obtain the optimal weighting factor, but σ_i^2 is unknown, and the following is based on the measurement value of each sensor to derive σ_i^2.

There are two mutually independent sensors i, j, the measured values are X_i, X_j, e_i, e_j is its measurement error, and X is the true value to be estimated. Then:

$$\begin{cases} X_i = X + e_i \\ X_j = X + e_j \end{cases} \tag{15}$$

Obviously, e_i, e_j are uncorrelated with each other and with X, and the mean value is 0. Therefore, their correlation coefficients R_{ij} are satisfied:

$$R_{ij} = E((X_i - \mu_i)(X_j - \mu_j)) = E(X^2) - \mu^2 \tag{16}$$

The autocorrelation coefficient R_{ii} of X_i is satisfied:

$$R_{ii} = E((X_i - \mu_i)^2) = E(X^2) + E(e_i^2) - \mu^2 \tag{17}$$

From Equations (15)–(17):

$$\sigma_i^2 = E(e_i^2) = R_{ii} - R_{ij} \tag{18}$$

Let the number of sensor measurements be k and the time-domain estimate of R_{ii} be:

$$R_{ii}(k) = \frac{1}{k}\sum_{q=1}^{k} (X_i(q) - \mu_i)^2 = \frac{k-1}{k} R_{ii}(k-1) + \frac{1}{k}(X_i(k) - \mu_i)^2 \tag{19}$$

Likewise:

$$R_{ij}(k) = \frac{1}{k}\sum_{q=1}^{k}(X_i(q)-\mu_i)(X_j(q)-\mu_j) = \frac{k-1}{k}R_{ij}(k-1) + \frac{1}{k}(X_i(k)-\mu_i)(X_j(k)-\mu_j) \quad (20)$$

In Equations (19) and (20), μ_i, μ_j denote the mean value of the sampled data; it can be seen that the more measurements that are taken, the more accurate the estimate is.

Extending Equation (20) to n sensors, the mean value of the correlation coefficient between two sensors is used as the estimated value of R_{ij}:

$$R_{ij} = \overline{R}_{ij}(k) = \frac{1}{n-1}\sum_{\substack{j=1 \\ j\neq i}}^{n} R_{ij}(k) \quad (21)$$

In this way, the time-domain estimates of the values to R_{ii}, R_{ij} are measured with each sensor [26], thus calculating the estimated variance σ_i^2 for each sensor.

2.6. Second-Level Convergence Based on LMBP Networks

The basic idea of the BP algorithm is that the learning process consists of two processes: signal forward propagation and error back propagation [27]. Through error back propagation, the weights of each layer are continuously adjusted until the error of the network output is reduced to an acceptable level, or the learning process is carried out to the end of a set number of times. The BP network consists of three layers: the input layer, the hidden layer, and the output layer, which are connected by full connection to build a communication bridge between neurons so that the data information can be connected one by one like multiple neurons for signaling and optimization for many iterations, and the weights of the neurons can be adjusted to achieve different prediction results of the output layer.

The traditional BP algorithm is based on first-order gradient descent, which is slow to converge and easy to fall into a local minimum. To solve the problems of the traditional BP algorithm, the LM algorithm (Levenberg–Marquardt) based on approximate second-order derivatives is used for optimization. The LM algorithm is a combination of gradient descent and Newton's method, with high accuracy, and the convergence time is greatly shortened compared to the gradient descent. The formula for adjusting the weights of the LMBP network is:

$$\omega_{k+1} = \omega_k - (J^T J + \mu I^{-1})J^T e \quad (22)$$

In Equation (22), ω_{k+1} is the weights of the $(k+1)$th iteration; J is the Jacobian matrix derived from the weights by the error vector e; and I is the unit matrix.

The following Figure 4 is a schematic diagram of a simple model of a neural network.

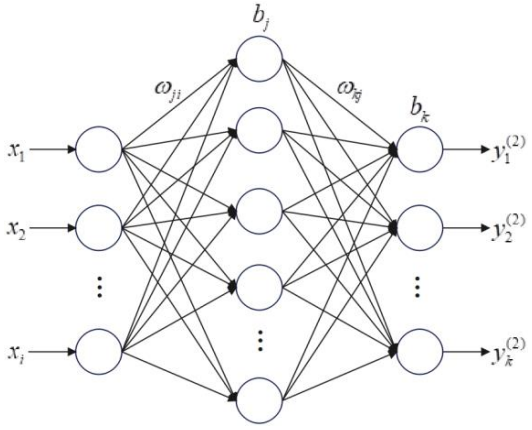

Figure 4. Schematic diagram of BP neural network.

The following is the process of building the neural network model:

1. Determine the number of layers of the BP network. The number of layers of the BP network depends on the demand, generally in a single layer of the network, and the number of neuron nodes can be increased. However, in this paper, the number of samples is large, and in order to reduce the size of the network and improve the output accuracy, multi-layer passes are added to the implicit layer.
2. Determine the number of hidden-layer nodes. Hidden-layer neurons affect the accuracy of the prediction results, and the number of neurons is determined using the trial-and-error method:

$$M = \sqrt{m+n} + \alpha \tag{23}$$

In Equation (23), M, m, n are the number of neurons in the hidden layer, input layer, and output layer, respectively; α is a constant value ranging from $\alpha \in [0, 10]$.

3. Determine the transfer function and learning algorithm. Taking a single-layer neural network as an example, the transfer formula from the input layer to the hidden layer is as follows:

$$y_j^{(1)} = f(\sum_{p=1}^{i} \omega_{jp} x_p + b_j) \tag{24}$$

In Equation (24), $y_j^{(1)}$ is the output of the i–th node of the hidden layer, and ω_{ji} is the transfer weight between the input layer and the hidden layer, if the propagation continues:

$$y_k^{(2)} = f(\sum_{q=1}^{j} \omega_{kq} y_q^{(1)} + b_k) \tag{25}$$

In Equation (25), q is the number of nodes in the implicit layer. If $y_k^{(2)}$ is the output of the last layer, then the output y_k is obtained from the 2-layer transfer of the input layer. The process of forward transfer introduces a nonlinear function $f(z)$; $f(z)$ is known as the activation function, and the commonly used Sigmoid function is the activation function:

$$f(z) = \frac{1}{1+e^{-z}} \tag{26}$$

The most rapid descent method is commonly used to adjust the BP network weights: the model is made to be adjusted in reverse layer by layer along the network to minimize the loss function, and the weights are iteratively updated to make the network track the effective data effectively to approach the target output. In this modeling, firstly, a large amount of basic data is provided for the neural network to establish a collection of neural networks for data classification, and finally, the probability under different conditions is obtained through the Softmax regression model [28].

The Softmax function is often used in the output layer of the multi-classification problem, which converts the original output value into a probability distribution, and each output can be interpreted as a probability that sums up to 1, which not only constructs the neuron output into a probability distribution but also plays the role of normalization [29]. And, the derivative of the Softmax function, i.e., the gradient of the function, is relatively easy to calculate, which makes it simple to use the gradient descent algorithm in the training process and makes the Softmax method more suitable for classification problems that require normalization processing. Therefore, in this classification model, the output of the Softmax function can effectively represent the judgment of the network model on the classification of evaluation indicators; D-S theory incorporates the probability of different decision factors, and the Softmax function solves the problem of the difficulty of assigning the basic probability in the practical use of D-S theory.

The evaluation indexes of the neural network classification model are chosen as the root mean square error *RMSE* and the coefficient of determination R^2. The standard root mean square error reflects the discrepancy between the model output value and the actual value, and the R^2 represents the nonlinear fitting characteristics of the model and the classification accuracy.

$$RMSE = \sqrt{\sum_{i=1}^{N} (y_i^* - y_i)/N} \tag{27}$$

$$R^2 = 1 - \sum_{i=1}^{N} (y_i^* - y_i)^2 / \sum_{i=1}^{N} (y_i^* - \overline{y})^2 \tag{28}$$

where y_i is the experimental value, y_i^* is the model output value, $\overline{y}$ is the average of the experimental values, and N is the number of samples in the data set.

2.7. Third-Level Fusion Based on Improved D-S Theory

2.7.1. Principle of D-S Theory

In 1967, Dempster proposed the D-S theory [30,31], which was further investigated by his student Shafer and described as follows:

Suppose that the full range of possible states of a discriminating object is the discriminating frame Θ, and the set consisting of all subsets of Θ is denoted as 2^Θ. If the function m:$2^\Theta \rightarrow$ [0, 1] satisfies Equation (29), then m is said to be the basic probability distribution function on Θ.

$$\begin{cases} \sum\limits_{A \subseteq 2^\Theta} m(A) = 1 \\ m(\varnothing) = 0 \end{cases} \tag{29}$$

where A is an arbitrary subset of Θ. A is said to be a focal element if $m(A) > 0$.

Suppose m_1, m_2,. . ., m_n are the basic probability distribution functions on the identification frame Θ. For $\forall A_1, A_2, \ldots, A_n \in 2^\Theta$, the D-S synthesis rule is as follows:

$$m(A) = \begin{cases} 0 & A = \varnothing \\ \dfrac{\sum\limits_{A_1 \cap A_2 \cap \ldots \cap A_n = A} \prod\limits_{i=1}^{n} m_i(A_i)}{1-K} & A \neq \varnothing \end{cases} \tag{30}$$

$$K = \sum_{A_1 \cap A_2 \cap \ldots \cap A_n = \varnothing} \prod_{i=1}^{n} m_i(A_i) \tag{31}$$

where K is the conflict coefficient, which indicates the degree of conflict between the pieces of evidence.

2.7.2. Improvement of D-S Theory in the Fusion of Environmental Information from Multiple Greenhouses

When the conflict coefficient K is less than the set value, the traditional D-S theory is used to fuse the environmental information from multiple greenhouses; when K is greater than the set value, the improved D-S theory is used as follows:

1. The mean value of each greenhouse for the j–th environmental evaluation is:

$$\overline{m}_j = \sum_{i=1}^{n} m_{ij}/n \tag{32}$$

   where n is the number of greenhouses divided.

2. The distance of the i–th greenhouse to the mean value of the said environmental evaluation is:

$$d_i = e^{-|m_{i1} - \overline{m}_1|} + e^{-|m_{i2} - \overline{m}_2|} + \ldots + e^{-|m_{ij} - \overline{m}_j|} \tag{33}$$

where m_{ij} is the basic probability assignment (BPA) of the i–th greenhouse to the j–th environmental assessment.

3. The weight of the i–th greenhouse environmental evaluation information is:

$$\omega_i = \frac{d_i}{\sum_{i=1}^{n} d_i} \tag{34}$$

4. The basic probability of a new environmental evaluation factor is:

$$\overline{m}'_j = \sum_{i=1}^{n} \omega_i m_{ij} \tag{35}$$

In Equation (35), $\sum_{i=1}^{n} \sigma_i = 1$.

3. Results

Potatoes have different requirements for environmental parameters at different fertility stages, and the LMBP network should be trained by fertility stages [32]. The tuber formation stage is the key period for determining the number of tubers, and the feasibility of the three-level fusion algorithm is verified by taking the tuber formation stage of the spring potato as an example.

3.1. Data Acquisition and Preprocessing

During the tuber formation period, the potato requires strong light—more than 16 h of sunlight conditions—and the aboveground part is optimally at 18–21 °C; if the temperature is too high and the light is insufficient, the leaves are large and thin, the stems elongate and become thin, and there is a collapse, which reduces the yield.

According to the actual situation, three homogeneous sensors were deployed in each greenhouse for air temperature, humidity, and light intensity, and the parameters were updated simultaneously every 1 min to monitor the growth environment of the potato in real time. The indoor air temperature data recorded in shed No. 1, 2, and 3 of the base on 5 June 2023 were used, and each greenhouse measured the temperature 10 times with three sensors in 10 min. The raw data from one of the sensors were as follows (Table 1):

Table 1. Raw data from an air temperature sensor.

Numbers	**1**	**2**	**3**	**4**	**8**	**9**	**7**	**8**	**9**	**10**
Temperature/(°C)	20.8	20.3	19.9	20.4	20.8	20.5	20.7	20.4	20.5	20.6

Sorting the raw data from smallest to largest yields gives the following: 19.9, 20.3, 20.4, 20.4, 20.5, 20.5, 20.6, 20.7, 20.8, 20.8. The upper quartile Q_3 = 20.65, the lower quartile Q_4 = 20.4, and the inter-quartile spacing IQR = 0.25, at which point data less than 20.025 or greater than 21.025 are anomalous. Among them, the third measurement of 19.9 is less than the lower limit value of 20.025, which is considered an outlier and is replaced with the mean value of the remaining data, which is 20.56.

It can be seen that the box-and-line diagram method can accurately identify the abnormal sample points, and these values are replaced with the mean value of the remaining data, which can still ensure the integrity of the data at the time of three-level fusion after cleaning and can effectively reduce the impact of abnormal values on prediction accuracy.

3.2. Adaptive Weighted Fusion Homogeneous Sensors

In the traditional adaptive weighting algorithm, the time-domain method is often used to calculate the variance of each sensor, but it is prone to anomalies such as variance < 0 and weights not converging in the process. In this paper, after rigorous derivation and

debugging of the adaptive weighting algorithm, the adaptive weighting algorithm has good results regardless of whether the truth value to be estimated changes with time.

Taking the three air temperature sensors in shed No.1 as an example, the air temperature fusion was measured 10 times continuously for 10 min.

The weights of each sensor converge when a certain number of measurements is reached, and the temperature weights have stabilized when the number of measurements is 10 and finally converge at 0.09, 0.25, and 0.66, respectively. After the weights converge, the estimated variance of each temperature sensor is 0.18, 0.05, and 0.03, and the total mean square error after fusion is 0.02, which meets the condition of minimizing the total mean square error and improves the data acquisition accuracy, which verifies the feasibility of the algorithm.

In the end, the adaptive weighted fusion result $\hat{X}$ was 20.54 °C. The indoor ambient temperature was in the optimal temperature range for the tuber formation stage, and no adjustment was needed. It is necessary to check whether sensor No. 1, which has a lower weight assignment, is faulty.

3.3. LMBP Network Fusion of Heterogeneous Sensors

After field visits by agronomic experts and an extensive literature review, 490 sets of environmental data during the tuber formation period were collected as a sample set, and the network was trained using Matlab 2023b [33,34].

The sample data were normalized to the interval [0, 1] using the MAPMINMAX() function before training. The normalized data were randomly disrupted with the RANDPERM() function, 350 groups of samples were randomly selected in the ratio of 7:3 for training the BP neural network, and 140 groups of samples were used to test the prediction effect of the model.

The newff() function was used to create the BP neural network, and the three-dimensional feature vector (air temperature, air humidity, light intensity)^{T} of the 350 groups of training samples was used as the input layer component, corresponding to the three neuron nodes in the input layer; the output component was the potato growth environment evaluation level, using the unique heat coding where "suitable", "uncertain", or "unsuitable" corresponds to "100", "010", or "001", so the number of nodes in the output layer is three. The initial value of the number of neuron nodes in the hidden layer is three, the termination value is 13, the step size is one, and the other parameters are fixed by the calculation of Equation (23) parameters. The step-by-step test is used to compare the prediction performance of each neural network, and finally, the neural network performance is best when the number of neuron nodes in the implied layer is 10.

The hidden layer is called the Sigmoid function, and the output layer is called the Softmax function. The trainlm function of the Levenberg–Marquardt algorithm is used as the training function [35] with 1000 iterations, an expected error of 1×10^{-6}, and a learning rate of 0.01.

As can be seen from Figure 5, the error converges progressively, and the iteration reaches the preset error requirement at the 18th cycle, the learning iteration of the LMBP network is aborted, the training time is 5 s, and the model has a high prediction accuracy and a fast computing speed.

After normalization of the dataset, the established LMBP network classification model is input, trained, and tested several times. The mean square error *RMSE*s of suitable, uncertain, and unsuitable are 0.15, 0.22, and 0.17, respectively, all within 0.25. The *RMSE*s of suitable and unsuitable are below 0.2, and the overall error accuracy is small. The coefficients of determination R^2 are 0.94, 0.88, and 0.91, respectively, all of which are more than 0.8, and the model has a high goodness of fit and is less affected by the nonlinear changes of environmental parameters. In summary, the established network model can effectively categorize the evaluation levels.

According to the monitored data, the potato growing environment is regulated through drip irrigation and other means to provide a suitable environment for potato development so as to ensure that the potato can grow normally.

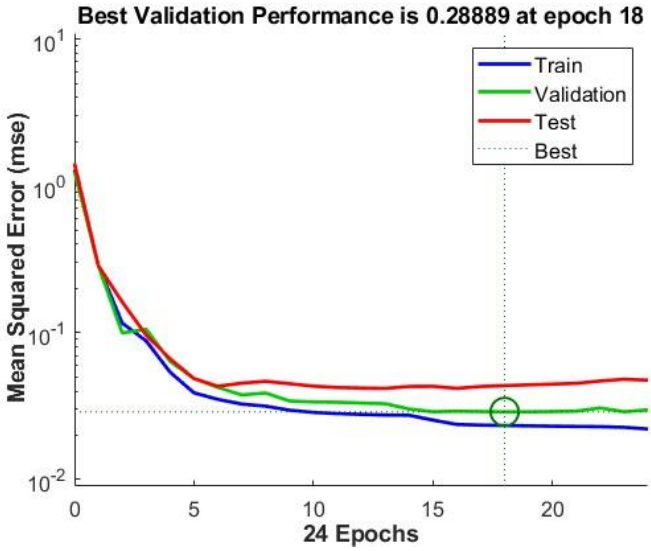

Figure 5. LMBP algorithm training error decline curve.

3.4. Improved D-S Theory Decision-Making

The adaptive fusion values of the three environmental factors were input into the LMBP network to obtain evidence of the independence of the three greenhouses, as shown in Table 2.

Table 2. Probability assignments for each greenhouse evaluation indicator.

Greenhouse Information	Suitable	Uncertain	Unsuitable
greenhouse 1	0.68	0.26	0.03
greenhouse 2	0.52	0.28	0.20
greenhouse 3	0.27	0.55	0.18

The conflict coefficient $K = 0.862328$ was calculated by Equation (31), which was larger than the preset value, and at the same time, the uncertain BPA of greenhouse 3 in Table 2 was the highest, which conflicted with the other two greenhouses, so it was fused by the improved D-S algorithm in this paper.

According to Equation (32), the mean value of each greenhouse for environmental evaluation was calculated, and the mean value $\overline{m}_1$ for "suitable" was 0.49, the mean value $\overline{m}_2$ for "uncertain" was 0.36, and the mean value $\overline{m}_3$ for "unsuitable" was 0.15. The distance from each greenhouse to the mean value of the environmental evaluation is calculated from Equation (33), giving $d_1 = 2.65$, $d_2 = 2.84$, and $d_3 = 2.60$, and the weights of the environmental information of each greenhouse are calculated from Equation (34). The new allocation probability is calculated according to Equation (35), replacing the conflicting allocation probability of greenhouse 3, and the new basic probability allocation function is shown in Table 3.

Table 3. New basic probability distribution function.

Greenhouse Information	Suitable	Uncertain	Unsuitable
greenhouse 1	0.68	0.26	0.03
greenhouse 2	0.52	0.28	0.20
greenhouse 3	0.4928	0.3598	0.1474

The combination of each greenhouse evidence in Table 2 from Equation (30) yields Table 4.

Table 4. Potato growing environment evaluation of fusion results.

Environmental Decision-Making	Suitable	Uncertain	Unsuitable
D-S theory	0.6934	0.2909	0.0157
Improved D-S theory	0.8836	0.1074	0.0090

As can be seen from Tables 3 and 4, compared with the LMBP network and the traditional D-S theory, the improved D-S theory greatly reduces the probability of the "uncertain" indicators, enhances the correlation between the monitoring indicators, and effectively improves the accuracy of the environmental evaluation results.

4. Conclusions

1. Adaptive weighting directly processes the raw data, which has the largest processing volume and the lowest anti-interference and fault-tolerance performance among the three levels of fusion, and its importance is self-evident. The environmental data are updated frequently and change little during the sampling time selected in this paper, and the outliers are removed by the box-and-line diagram method and filled by the mean value, which reduces the interference of outliers on the fusion without affecting the integrity of the data. The measured values of air temperature, humidity, and light intensity are unbiased estimates of the true value to be estimated. After fusion, the total error is less than the error of each individual sensor, giving us the best estimate of each measurement. Sensor weights are assigned based on their variance and adjusted as needed. Their significance in greenhouse environmental monitoring is that the higher the measurement accuracy, the closer to the overall performance of the sensor and the lower the variance, so the allocation of higher weights makes the fusion results that are not due to individual sensor failures appear to be larger deviations. The allocation of lower-weight sensors needs to be overhauled in a timely manner.
2. The application of D-S theory is difficult in basic probability allocation. This paper proposes a combination of an LMBP network and an improved D-S theory. The process of obtaining the environmental factors on the evaluation-level BPA is complex: making full use of the BP network self-learning function, the output layer selects the Softmax function and the hidden-layer output variables into the probability of [0, 1] intervals, and after training, the BP network has a strong generalization ability to describe this complex nonlinear relationship. Compared with the traditional D-S theory, the improved D-S theory reduces the probability of "uncertain" indicators in the fusion results. By applying this method to the environmental monitoring of potato growth in a continuous greenhouse, the fusion of uncertain information has a strong robustness.
3. In this paper, information fusion technology is introduced into the potato growth control system, and a multilevel fusion framework—including a data level, a feature level, and a decision level—is constructed, whose robustness meets the comprehensive analysis of the collected data in the greenhouse and achieves good results in predicting the growth and development of potatoes. On the one hand, the environmental conditions of potatoes in different greenhouses often do not differ much, and it is important to analyze the changes in the decision-level fusion results over time. The output of the decision-level fusion facilitates the user to intuitively control the environmental conditions of multiple greenhouses and to generally schedule agricultural activities, which reduces the consumption of manpower and material resources in batch scheduling and is especially important for the efficient cultivation of large-scale continuous greenhouse crops.

   On the other hand, if an environmental factor deviates slightly from the optimal value suitable for potato growth, this does not mean that environmental regulation should

be carried out immediately because environmental decisions are influenced by multiple factors, and single-threshold control can cause economic losses. Regulation should only occur if the greenhouse feature-level fusion result is 'unsuitable'. This approach maintains fusion accuracy while reducing data processing. The fusion results are stored and used as the yield analysis of the potato smart farm platform, providing a scientific basis for precise greenhouse control. Potatoes prefer cold, while for other greenhouse cash crops, controlling energy-saving hot-air furnaces and sunlight lamps and regulating other environmental parameters until they meet the requirements has a better effect.

Author Contributions: Conceptualization, S.L. and T.Z.; methodology, S.L.; software, S.L.; validation, S.L.; formal analysis, S.L.; investigation, S.L.; resources, S.L.; data curation, S.L.; writing—original draft preparation, S.L.; visualization, S.L.; writing—review and editing, H.Z., J.Z., Z.P. and R.Y.; supervision, R.Y.; project administration, R.Y.; funding acquisition, R.Y. All authors have read and agreed to the published version of the manuscript.

Funding: This research was funded by the Hainan Provincial Postgraduate Innovative Research Project (Qhys2022-135).

Institutional Review Board Statement: Not applicable.

Data Availability Statement: The original contributions presented in the study are included in the article, further inquiries can be directed to the corresponding author.

Conflicts of Interest: The authors declare no conflicts of interest.

References

1. Huo, W.; Crants, J.E.; Miao, Y.; Rosen, C.J. Impact of Phosphorus Rate, Soil Fumigation, and Cultivar on Potato Yield, Quality, Phosphorus Use Efficiency and Economic Returns in a High Phosphorus Soil. *Eur. J. Agron.* **2024**, *153*, 127069. [CrossRef]
2. Pinem, M.I.; Lubis, L.; Marheni; Zuhdi, D.M. The Effect of a Combination of Growing Media and Biological Agents to Control Bacterial Wilt Disease of Potato (Ralstoniasolanacearum) in Greenhouse. *J. Phys. Conf. Ser.* **2020**, *1485*, 012031. [CrossRef]
3. Ono, S.; Yasutake, D.; Kimura, K.; Kengo, I.; Teruya, Y.; Hidaka, K.; Yokoyama, G.; Hirota, T.; Kitano, M.; Okayasu, T.; et al. Effect of Microclimate and Photosynthesis on Strawberry Reproductive Growth in a Greenhouse: Using Cumulative Leaf Photosynthesis as an Index to Predict the Time of Harvest. *J. Hortic. Sci. Biotechnol.* **2024**, *99*, 223–232. [CrossRef]
4. Gong, L.; Yu, M.; Kollias, S. Optimizing Crop Yield and Reducing Energy Consumption in Greenhouse Control Using PSO-MPC Algorithm. *Algorithms* **2023**, *16*, 243. [CrossRef]
5. Shi, J.; Li, M.; Tong, B.; Guo, Z. A New Control Strategy for Greenhouse Environment Control System Based on Inverse Model. *Int. J. Heat Technol.* **2022**, *40*, 1271–1276. [CrossRef]
6. Morcego, B.; Yin, W.; Boersma, S.; Van Henten, E.; Puig, V.; Sun, C. Reinforcement Learning versus Model Predictive Control on Greenhouse Climate Control. *Comput. Electron. Agric.* **2023**, *215*, 108372. [CrossRef]
7. Qiao, D.; Zhang, Z.; Liu, F.; Sun, B. Location Optimization Model of a Greenhouse Sensor Based on Multisource Data Fusion. *Complexity* **2022**, *2022*, 3258549. [CrossRef]
8. Rosero-Montalvo, P.D.; Erazo-Chamorro, V.C.; López-Batista, V.F.; Moreno-García, M.N.; Peluffo-Ordóñez, D.H. Environment Monitoring of Rose Crops Greenhouse Based on Autonomous Vehicles with a WSN and Data Analysis. *Sensors* **2020**, *20*, 5905. [CrossRef] [PubMed]
9. Benghanem, M.; Mellit, A.; Khushaim, M. Environmental Monitoring of a Smart Greenhouse Powered by a Photovoltaic Cooling System. *J. Taibah Univ. Sci.* **2023**, *17*, 2207775. [CrossRef]
10. Lei, W.; Lu, H.; Qi, X.; Tai, C.; Fan, X.; Zhang, L. Field Measurement of Environmental Parameters in Solar Greenhouses and Analysis of the Application of Passive Ventilation. *Sol. Energy* **2023**, *263*, 111851. [CrossRef]
11. Xu, B. Research on Indoor Environment Positioning System Considering Multisensor in the Multi-Information Data Fusion. *Mob. Inf. Syst.* **2022**, *2022*, 1676155. [CrossRef]
12. Mirzaei, A.; Bagheri, H.; Sattari, M. Data Level and Decision Level Fusion of Satellite Multi-Sensor AOD Retrievals for Improving PM2.5 Estimations, a Study on Tehran. *Earth Sci. Inform.* **2023**, *16*, 753–771. [CrossRef]
13. Perez, S.; Maddu, S.; Sbalzarini, I.F.; Poncet, P. Adaptive Weighting of Bayesian Physics Informed Neural Networks for Multitask and Multiscale forward and Inverse Problems. *J. Comput. Phys.* **2023**, *491*, 112342. [CrossRef]
14. Pathak, G.S.; Singh, S.K.; Singh, C.P. Effect of Different Date of Planting and Various Mulching Practices on Growth, Yield Attributes and Yield of Potato. *Int. J. Plant Soil Sci.* **2024**, *36*, 279–286. [CrossRef]
15. Hwang, J.; Lee, S.; Lee, J.-H.; Kang, W.-H.; Kang, J.-H.; Kang, M.-Y.; Oh, C.-S.; Kang, B.-C. Plant Translation Elongation Factor 1Bβ Facilitates Potato Virus X (PVX) Infection and Interacts with PVX Triple Gene Block Protein 1. *PLoS ONE* **2015**, *10*, e0128014. [CrossRef] [PubMed]

16. Rumiantsev, B.; Dzhatdoeva, S.; Sadykhov, E.; Kochkarov, A. A Model for the Determination of Potato Tuber Mass by the Measurement of Carbon Dioxide Concentration. *Plants* **2023**, *12*, 2962. [CrossRef] [PubMed]
17. Samanta, S.; Banerjee, S.; Mukherjee, A.; Patra, P.K.; Chakraborty, P.K. Determining the Radiation Use Efficiency of Potato Using Sunshine Hour Data: A Simple and Costless Approach. *Span. J. Agric. Res.* **2020**, *18*, e0801. [CrossRef]
18. Gikundi, E.N.; Buzera, A.; Orina, I.; Sila, D. Impact of the Temperature Reconditioning of Cold-Stored Potatoes on the Color of Potato Chips and French Fries. *Foods* **2024**, *13*, 652. [CrossRef] [PubMed]
19. Jaber, Z.K.; Oleiwi, M.S. The Effect of Biofertilizers, Phosphorus Sources and Vermicompost on the Preparation of Bacterial and Fungal Cells for the Two Phases of Vegetative Growth and Flowering of Potato Plants. *IOP Conf. Ser. Earth Environ. Sci.* **2023**, *1262*, 082040. [CrossRef]
20. Nemec, D.; Andel, J.; Simak, V.; Hrbcek, J. Homogeneous Sensor Fusion Optimization for Low-Cost Inertial Sensors. *Sensors* **2023**, *23*, 6431. [CrossRef]
21. Sun, Y.; Shi, Y. Adaptive Self-Triggered Control-Based Cooperative Output Regulation of Heterogeneous Multi-Agent Systems under Sensor and Actuator Attack. *Proc. Inst. Mech. Eng. Part J. Syst. Control Eng.* **2024**, *238*, 59–72. [CrossRef]
22. Li, J.; Liang, W.; Yin, X.; Li, J.; Guan, W. Multimodal Gait Abnormality Recognition Using a Convolutional Neural Network–Bidirectional Long Short-Term Memory (CNN-BiLSTM) Network Based on Multi-Sensor Data Fusion. *Sensors* **2023**, *23*, 9101. [CrossRef]
23. Liu, Z.; Yao, L.; Cao, L.; Liang, H. Distributed Event-Triggered Control for Multiagent Systems with Non-Continuous Communication Faults and Dynamic Uncertainties. *Nonlinear Dyn.* **2022**, *110*, 1501–1514. [CrossRef]
24. Chen, Y.; Zhang, H.; Liu, M.; Ye, M.; Xie, H.; Pan, Y. Traffic Signal Optimization Control Method Based on Adaptive Weighted Averaged Double Deep Q Network. *Appl. Intell.* **2023**, *53*, 18333–18354. [CrossRef]
25. Lu, P.; Yang, J.; Ye, L.; Zhang, N.; Wang, Y.; Di, J.; Gao, Z.; Wang, C.; Liu, M. A Novel Adaptively Combined Model Based on Induced Ordered Weighted Averaging for Wind Power Forecasting. *Renew. Energy* **2024**, *226*, 120350. [CrossRef]
26. González-Hidalgo, M.; Massanet, S.; Mir, A.; Ruiz-Aguilera, D. Impulsive Noise Removal with an Adaptive Weighted Arithmetic Mean Operator for Any Noise Density. *Appl. Sci.* **2021**, *11*, 560. [CrossRef]
27. Li, Z.; Qiu, X.; Yang, J.; Meng, D.; Huang, L.; Song, S. An Efficient BP Algorithm Based on TSU-ICSI Combined with GPU Parallel Computing. *Remote Sens.* **2023**, *15*, 5529. [CrossRef]
28. Jawa, T.M.; Fatima, N.; Sayed-Ahmed, N.; Aldallal, R.; Mohamed, M.S. Residual and Past Discrete Tsallis and Renyi Extropy with an Application to Softmax Function. *Entropy* **2022**, *24*, 1732. [CrossRef] [PubMed]
29. Shao, H.; Wang, S. Deep Classification with Linearity-Enhanced Logits to Softmax Function. *Entropy* **2023**, *25*, 727. [CrossRef]
30. Bisht, K.; Kumar, A. Stock Portfolio Selection Hybridizing Fuzzy Base-Criterion Method and Evidence Theory in Triangular Fuzzy Environment. *Oper. Res. Forum* **2022**, *3*, 53. [CrossRef]
31. Zhang, Y.; Yan, W.; Hong, G.S.; Fuh, J.F.H.; Wang, D.; Lin, X.; Ye, D. Data Fusion Analysis in the Powder-Bed Fusion AM Process Monitoring by Dempster-Shafer Evidence Theory. *Rapid Prototyp. J.* **2022**, *28*, 841–854. [CrossRef]
32. Li, C.; Ma, C.; Chen, P.; Cui, Y.; Shi, J.; Wang, Y. Machine Learning-Based Estimation of Potato Chlorophyll Content at Different Growth Stage Using UAV Hyperspectral Data. *Zemdirb.-Agric.* **2021**, *108*, 181–190. [CrossRef]
33. Lautre, R.; Sadawarti, M.J.; Lekhi, R.; Samadhiya, R.K.; Singh, S.P.; Dangi, R.S.; Kumar, V.; Verma, D.; Patidar, P. Performance of Short-Duration Potato (*Solanum tuberosum* L.) Hybrids and Varieties for Growth and Yield Attributing Characteristics in Chambal Region of Madhya Pradesh, India. *Int. J. Environ. Clim. Change* **2023**, *13*, 2019–2032. [CrossRef]
34. Mthembu, S.G.; Magwaza, L.S.; Mashilo, J.; Mditshwa, A.; Odindo, A. Drought Tolerance Assessment of Potato (*Solanum tuberosum* L.) Genotypes at Different Growth Stages, Based on Morphological and Physiological Traits. *Agric. Water Manag.* **2022**, *261*, 107361. [CrossRef]
35. Sundar, L.S.; Chandra Mouli, K.V.V. Experimental Analysis and Levenberg-Marquardt Artificial Neural Network Predictions of Heat Transfer, Friction Factor, and Efficiency of Thermosyphon Flat Plate Collector with MgO/Water Nanofluids. *Int. J. Therm. Sci.* **2023**, *194*, 108555. [CrossRef]